The United Nations University

GEOTHERMAL TRAINING PROGRAMME
Orkustofnun, Grensásvegur 9,
IS-108 Reykjavík, Iceland

Reports 2004
Number 17

APPLICATION OF GEOCHEMICAL METHODS IN LOW-TEMPERATURE GEOTHERMAL AREAS: STRANDIR AREA, NW-ICELAND AND THE LIANGXIANG FIELD, BEIJING, CHINA

Xu Wei
Beijing Institute of Geological Engineering
Geothermal Engineering Department
90 Beiwa Road, Haidian District
100037 Beijing
P.R. CHINA
xuwei_2004_26@263.net

ABSTRACT

Geochemistry plays an important role during exploration, drilling and later development of geothermal resources. A few geochemical methods are introduced and applied to the two low-temperature geothermal areas, namely Strandir area in NW-Iceland and the Liangxiang field, Beijing, China. The Chebotarev diagram and the Cl-SO_4-HCO_3 ternary diagram are used to classify natural waters. Most fluids in the reservoirs of the Strandir area are chlorite-bicarbonate waters except the Drangsnes field, which belongs to chlorite waters. The fluid in the reservoir of the Liangxiang field is classified as bicarbonate waters. Several kinds of geothermometers are calculated to predict the subsurface temperatures. Chalcedony and Na/K geothermometers show the range 22-100°C in the Strandir area, and the subsurface temperature in the Liangxiang field is 43-56°C by the chalcedony geothermometers. As for mixing, the Schoeller diagram and silica-enthalpy mixing model are used, indicating that the fluids in the Strandir area have been mixed with cold water, but no mixing with groundwater has occurred in the Liangxiang field. In addition, the valuation of mineral-solution equilibrium is discussed by a log (Q/K) diagram. Most of fluids in both areas are not in equilibrium with minerals.

1. INTRODUCTION

Geothermal exploration serves the purpose of locating geothermal areas favourable to development and to finding sites within them for drilling. This exploration includes geological mapping as well as geochemical and geophysical surveys. The principal purpose of geochemical surveys is to predict subsurface temperatures, to obtain information on the origin of the geothermal fluid and to understand subsurface flow directions. In addition, geochemistry plays an important role during geothermal exploration drilling and later development of geothermal reservoirs. It can furnish data on the chemical properties of the discharged fluid in wells, which contribute to the overall understanding of the production characteristics of the geothermal reservoir. After production has been initiated, geochemical monitoring is one of the most useful tools to predict the response of the reservoir to the

production load, including recharge, pressure drawdown and scaling or corrosion tendencies. In this paper, a few geochemical methods will be introduced, including classifications of natural water, geothermometry, mixing models, mineral-solution equilibria and interpretation of monitoring of chemical components, which have been used widely in Iceland.

Vestfirdir, or the Westfjords, is a peninsula located in the northwest part of Iceland. There are many low-temperature hot springs distributed in the area and some wells have been drilled during the primary exploration. This paper will concentrate on the Strandir area in the eastern part, where limited exploration has been done. Some data samples exist from hot springs and boreholes, collected in the 1970's, and were dealt with by geochemical methods. The interpretation of these samples from the different locations can show the chemical properties of fluids in their reservoirs.

The Liangxiang field, located in the Fangshan district, Beijing, is rich in low-temperature geothermal resources. It is more than 30 years since the first exploration well was drilled near Yutian Tower in the 1960's. In the past, some surveys of the geothermal resources in this field have been carried out, and monitoring has also been continued. So far, more than 20 geothermal exploration wells with depth of 800-1500 m and temperature range of 36-60ºC have been drilled in the field, and the area of resources assessed extends to 68 km^2 (Xiang et al., 2000). Geochemical methods will be applied to a few samples from this field in order to assess the chemical properties of the fluid in the reservoir and predict the response of the reservoir to production during exploitation in the future.

This report can be divided into three main parts:

- Introduction to geochemical methods;
- Application of the methods to the Strandir low-temperature geothermal area, NW-Iceland;
- Assessment of the properties of the reservoir in the Liangxiang geothermal field, Beijing.

2. METHODOLOGY

2.1 Classification of the water

2.1.1 Chebotarev diagram

As far as natural waters are concerned, there are five fundamental geochemical types assuming that anions are independent parameters and cations are dependent, changing with the increase of the total salinity, namely bicarbonate waters, bicarbonate-chloride waters, chloride-bicarbonate waters, chloride-sulphate or sulphate waters, and chloride waters (Chebotarev, 1955). In order to put a high number of samples together and have quick visual control of the analogies and the differences between various samples or groups of samples, the diagram proposed by Chebotarev (1955) is preferred. The groups of anions and cations, significant from a geochemical point of view (Ca+Mg, Na+K, SO_4+Cl, CO_3+HCO_3) are transformed in reacting values in percentage, that is to say the ratio between the concentration of the above defined groups of cations and anions, and the sum of cations and anions respectively. The reaction values of both significant groups are recorded on the ordinates and abscissae, one increasing, the other decreasing, in such a way that the sum of the distances of the borderlines of the diagram is always a constant value equal to 50% for the cations and 50% for the anions. The waters which fall in the upper left area correspond to thermal waters with a high content of NaCl; the waters on the lower left side represent acid waters through oxidation of hydrogen sulphide to sulphuric acid without carbonates-bicarbonates; waters with lower values of salinity fall in the area of alkali bicarbonate-sulphate-chloride and not alkali earth bicarbonate chemistry (Dall´Aglio et al., 1972).

2.1.2 Cl-SO_4-HCO_3 ternary diagrams

Most geochemical techniques may with confidence be applied only to specified types of fluids with limited ranges of compositions. Any such interpretation of geothermal water samples, therefore, is best carried out on the basis of an initial classification. The Cl-SO_4-HCO_3 ternary diagram is one of the diagrams for the classification of natural waters (Giggenbach, 1988). The position of a data point in such a triangular or trilinear plot is simply obtained by first forming the sum S of the concentrations C_i (in mg/kg) of all three constituents involved.

$$S = C_{Cl}+C_{SO4}+C_{HCO3}$$

Then the percentage of each component can be calculated as X, Y, Z axis, respectively. In this diagram, composition ranges are indicated for several typical groups of waters such as volcanic and steam-heated waters, mature waters and peripheral waters. Normally, the group best suited comprises the neutral, low sulphate, high chloride 'geothermal' waters along the Cl-HCO_3 axis, close to the Cl corner, namely mature waters. In addition, not only can it be used to weed out unsuitable waters, but may provide an initial indication of mixing relationships or geographic groupings. For instance, the degree of separation between data points for high chloride and bicarbonate waters gives an idea of the relative degrees of interaction of CO_2 charged fluids at lower temperature, and of the HCO_3 contents increasing with time and distance travelled underground (Giggenbach, 1988).

Thus, it is important to classify the samples into different groups to control the relations of these samples in general, before further chemical studies. Compared to the Cl-SO_4-HCO_3 diagram, the Chebotarev diagram is an older method to classify the natural waters, but due to its advantage of simplicity and efficiency, it is still in use today in geothermal research in Beijing. The triangular diagrams devised later can classify the geothermal waters specially and weed out unsuitable waters to geochemical techniques (Giggenbach, 1988).

2.2 Geothermometry

Geothermometry is used to calculate and predict the potential of temperature for geothermal fluid. Water geothermometers may be broadly classified into two groups: (1) those which are based on temperature-dependent variations in solubility of individual minerals; and (2) those which are based on temperature-dependent exchange reactions which fix ratios of certain dissolved constituents (Fournier, 1989).

2.2.1 The silica geothermometers

The solubilities of all silica minerals decrease drastically as temperature decreases below 340ºC. The rate of dissolution and precipitation of quartz and amorphous silica changes as logarithmic functions of absolute temperature, with moderately fast rates at very high temperatures and extremely slow rates at low temperatures (Rimstidt and Barnes, 1980). Solutions become saturated with respect to a given silica mineral in a geothermal reservoir after prolonged water-rock interaction at a constant temperature, and therefore, little dissolved silica polymerizes and precipitates during relatively fast upward movement to the earth's surface. In general, significant amounts of silica precipitate from a given quantity of an ascending solution only when the solubility of amorphous silica is exceeded. At temperatures less than about 300ºC, and at depths generally attained by commercial drilling for geothermal resources, variations in pressure at hydrostatic conditions have little effect on the solubilities of quartz and amorphous silica (Fournier and Potter, 1982a; Fournier and Rowe, 1977); and added salt has a significant effect only at concentrations above about 2-3 wt% (Fournier, 1985; Fournier and Marshall, 1983).

The solubility of silica is also affected by variations in pH when pH is greater than about 7.5. When pH is less than about 2 to 3, acid attack upon alumino-silicates may effectively control dissolved silica concentrations at values above the solubilities of quartz and chalcedony, particularly where temperatures are less than about 100-150ºC. However, water-rock reactions generally fix the pH of reservoir fluids at values between 5.0 and 7.5, therefore corrections for effects of pH usually need not be made in silica geothermometer calculations. Considering all the above factors, dissolved silica concentrations in hydrothermal solutions with near neutral pH can generally be used as one of the more reliable chemical geothermometers (Fournier, 1989).

a) *Quartz geothermometers*

The solubility of quartz appears to control dissolved silica in geothermal reservoirs at temperatures higher than 120-180ºC, which is too high for low-temperature geothermal resources. Therefore, an equation (Fournier and Potter, 1982b) applicable over a much greater temperature range (20-330ºC) at the vapour pressure of the solution is selected, which is listed in Table 1.

TABLE 1: Equations for different geothermometers (°C)

Type of geothermometers	Equation	Range (°C)	Author
Quartz - no steam loss (T1)	$t = \frac{1309}{5.19 - \log S} - 273.15$	100-250	Fournier (1977)
Quartz - maximum steam loss at 100ºC	$t = \frac{1522}{5.75 - \log S} - 273.15$	100-250	Fournier (1977)
Quartz (20-330ºC)	$t = -42.2 + 0.28831S - 3.6686\times10^{-4}S^2 + 3.1665\times10^{-7}S^3 + 77.034 \log S$	20-330	Fournier and Potter (1982b)
Chalcedony (T2)	$t = \frac{1032}{4.69 - \log S} - 273.15$	0-250	Fournier (1977)
Na-K (T3)	$t = \frac{856}{0.857 + \log(Na/K)} - 273.15$		Truesdell (1976)
Na-K	$t = \frac{833}{0.780 + \log(Na/K)} - 273.15$		Tonani (1980)
Na-K (T4)	$t = \frac{933}{0.933 + \log(Na/K)} - 273.15$	25-250	Arnórsson et al. (1983)
Na-K (T5)	$t = \frac{1217}{1.483 + \log(Na/K)} - 273.15$		Fournier (1983)
Na-K (T6)	$t = \frac{1390}{1.75 + \log(Na/K)} - 273.15$		Giggenbach et al. (1983)
Na-K-Ca (T7)	$t = \frac{1647}{\log(Na/K) + ß\left[\log(\sqrt{Ca}/Na) + 2.06\right] + 2.47} - 273.15$ ß = 4/3 for t<100ºC; ß = 1/3 for t>100ºC		Fournier and Truesdell (1973)
K-Mg (T8)	$t = \frac{4410}{14.00 - \log(K^2/Mg)} - 273.15$		Giggenbach (1988)
Na-Ca (T9)	$t = \frac{1096.7}{3.080 - \log(Na/\sqrt{Ca})} - 273.15$		Tonani (1980)
K-Ca (T10)	$t = \frac{1930}{3.861 - \log(K/\sqrt{Ca})} - 273.15$		Tonani (1980)

S = concentration of SiO_2; Na = concentration of Na^+; K = concentration of K^+;
Mg = concentration of Mg^{2+}; Ca = concentration of Ca^{2+}.

b) *Chalcedony geothermometers*
There is ambiguity in the use of silica geothermometers at temperatures less than about 180ºC because chalcedony appears to control dissolved silica in some places, and quartz in others. Chalcedony is a very fine-grained variety of quartz composed of aggregates of very tiny crystals. The individual quartz grains are so small that they have relatively large surface energies compared to 'normal' quartz, and this results in an increase in solubility. Chalcedony is unstable in contact with water at temperatures above about 120-180ºC because the smallest sized crystals dissolve completely relatively quickly and larger sized crystals grow large enough so that surface energy is no longer a factor. Temperature, time, fluid composition, and prior history all affect the size attained by quartz crystals. Thus, in some places where water has been in contact with rock at a given temperature for a relatively long time, such as in some deep sedimentary basins, quartz may control dissolved silica at temperatures less than 100ºC. In other places, chalcedony may control dissolved silica at temperature as high as 180ºC. For this reason, it was recommended that both quartz and chalcedony silica geothermometer temperatures be calculated when reservoir temperature appeared to be less than 180ºC. The equations are listed in Table 1 (Fournier, 1989).

2.2.2 Cation geothermometers

Cation geothermometers are widely used to calculate subsurface temperature of waters collected from hot springs and wells. They are based on ion exchange reactions with temperature-dependent equilibrium constants.

a) *Na/K geothermometers*
Experiments at high temperature and pressure by Orville (1963) and Hemley (1967) showed that reactions involving base exchange of Na and K between alkali feldspars and solutions proceed very slowly at temperatures below about 300ºC. Also, where reservoir temperatures are changing in response to production, the Na/K geothermometer generally appears to take longer than the silica geothermometer to attain a new water-rock chemical equilibrium. Therefore, there is a tendency to use the Na/K ratio to estimate possible higher temperatures in deeper parts of a system where waters reside for relatively long periods of time (Fournier, 1989). The reaction formula of the exchange of Na^+ and K^+ between co-existing alkali feldspars is:

$$NaAlSi_3O_8 + K^+ = KAlSi_3O_8 + Na^+ \quad (1)$$

Assuming the activities of the solid reactions are unity and activities of the dissolved species are about equal to their molal concentrations in aqueous solution, the equilibrium constant K for this reaction is the ratio between the concentrations of Na and K. The variation of the equilibrium constant with temperature is given by an integrated form of the Van't Hoff equation:

$$\log K = \frac{\Delta H^\circ}{2.303RT} + C \quad (2)$$

where ΔH° = Differential heat of solution (enthalpy of the reaction);
T = Temperature (K);
R = Gas constant = 8.31 J/K mole; and
C = Constant of integration.

The value of ΔH° generally changes little with temperature in the range of 0-300ºC, therefore a plot of $\log K_{eq}$ versus $1000/T$ gives an approximately straight line (Fournier, 1989).

A few equations used to calculate the Na/K geothermometer temperature published by different authors are listed in Table 1. The reasons include that a considerable range in structural states of alkali feldspars may persist metastably at low temperature; base exchanges involve different kinds (structural states) of K-feldspar; also, other minerals may participate in cation exchange reactions involving Na

and K. So when the Na/K geothermometer is applied to hot-spring waters or waters from sedimentary basins, the results are probably too high because basic exchange reactions involving clays may control Na/K ratios there (Fournier, 1989).

b) *The Na-K-Ca geothermometer*
The Na-K-Ca geothermometer (Fournier and Truesdell, 1973) takes account of reactions involving exchange of Na^+, K^+ and Ca^{2+} with mineral solid solutions. The geothermometer is entirely empirical and assumes one type of base exchange at temperatures above about 100ºC:

$$K^+ + Na_{2/3}Ca_{1/6}\text{-solid} = (1/6)Ca^{+2} + (2/3)Na^+ + K\text{-solid} \quad (3)$$

And a different exchange reaction at temperatures below about 100ºC,

$$K^+ + (1/3)\ Na^+ + Ca_{2/3}\text{-solid} = (2/3)\ Ca^{+2} + K\ Na_{1/3}\text{-solid} \quad (4)$$

The general form of both of the above reactions is:

$$\log K = \log (Na/K) + ß \log (\sqrt{Ca} / Na) \quad (5)$$

where ß = ⅓ for waters equilibrating above approx. 100ºC; and
ß = ¾ for waters equilibrating below approx. 100ºC.

An exception to this rule is that ß equal to 1/3 should be used for waters less than 100ºC when log ($Ca^{1/2}$/Na) is negative, with concentrations of dissolved constituents expressed in molality units.

c) *Other cation geothermometers*
Various other cation geothermometers have been proposed that may be of use in some situations, including K^2/Mg (Giggenbach et al., 1983), Li^2/Mg (Kharaka and Mariner, 1989), Na/√Ca (Tonani, 1980), K/Ca (Tonani, 1980) and Na/Li (Fouillac and Michard, 1981; Kharaka et al., 1982) etc. Water-rock exchange reactions involving Mg proceed relatively fast at low temperatures, and K^2/Mg and Li^2/Mg ratios appear to be good indicators of the last temperature of water-rock equilibration in the ascending water. A contributing factor in this apparent fast re-equilibration is that both Mg and Li tend to be minor constituents in most thermal waters, thus a relatively small amount of reaction involving one or both of these constituents may have a large effect on the ratios of cations remaining in the solution. The problem of applying cation ratios involving Ca is the likelihood of it being affected by variations in CO_2 partial pressure. The Na/Li geothermometers appear to be particularly sensitive to total dissolved solids and to rock type, so it commonly yields very different results when applied to the same water.

d) *Na-K-Mg triangular diagram*
In terms of Na/K (Giggenbach et al., 1983) and slightly modified K^2/Mg geothermometer equations (Giggenbach et al., 1983), a triangular diagram with Na/1000, K/100, and √Mg at the apices can be used to classify waters as fully equilibrated with rock at given temperatures, partially equilibrated, and immature (Giggenbach, 1988). This method was devised to give an automatic indication as to the suitability of the given water for the application of ionic solute geoindicators. The temperatures and compositions at which 'full equilibration' may change significantly, depending on which of the many Na/K geothermometers one assumes to be correct and the mineralogy (including structural states) of the phases that are in contact with the reservoir fluid. The position of the full equilibrium line also changes as the assumed K_2/Mg geothermometer equation changes. Evaluation of the Na-K-Mg geothermometer is best carried out by use of the blank diagram provided by Giggenbach (1988).

In addition to eliminating the unsuitable samples and obtaining the degree of attainment of water-rock equilibrium to be assessed, the main advantage of this diagram is its ability to depict the position of a large number of samples simultaneously, permitting the delineation of mixing trends and groupings.

Also, the positions of waters resulting from the two end member processes, rock dissolution and equilibration, are well separated removing any doubt as to their relative importance in shaping the composition of a geothermal water.

2.3 Mineral-solution equilibrium

One of the assumptions of the chemical geothermometers presented above is the equilibrium between the fluid and minerals in the reservoir. A geothermal system is characterized by a flow of fluid through a body of rock. This fluid will react with the rock chemically and, as is the case with any chemical reaction, change the system towards equilibrium.

The thermodynamic properties of minerals and species change with temperature and pressure. The effect of temperature is much greater than the effect of pressure in the temperature range from 0 to 350ºC and pressure range from 1 to 200 bar, so the effect of pressure on mineral-solution equilibrium can be neglected. The equilibrium state for a given reaction of mineral and solution in a geothermal system can be evaluated by the value of the equilibrium constant (K) for the given reaction to the reaction quotient (Q).

The equilibrium constant, K, for a given reaction is calculated from the standard Gibbs energy of reaction, ΔGr^0, by:

$$\ln K = -\Delta Gr^0/RT \tag{6}$$

where R = Gas constant; and
T = Temperature (K).

The reaction quotient, Q, for the reaction is given by:

$$Q = \prod_i \frac{a_{i,m}^{v_{i,m}}}{a_m} \tag{7}$$

where $a_{i,m}$ = Activity of aqueous species i (in mole/kg);
$v_{i,m}$ = Stoichiometric coefficient of species i in the mineral; and
Activity of pure minerals = 1.

The Gibbs energy of reaction is relative to the reaction quotient through:

$$\Delta Gr = \Delta Gr^0 + RT \ln Q \tag{8}$$

Combination of Equations 6 and 8 yields:

$$\Delta Gr = -RT \ln K + RT \ln Q = RT \ln Q/K \tag{9}$$

Hence, at equilibrium, $K = Q$; for supersaturated solution, $Q > K$ and for undersaturated solution, $Q < K$ (Arnórsson, 2000).

Generally, calculation of aqueous speciation requires the use of aqueous speciation computer programs, such as WATCH (Arnórsson et al., 1983; Bjarnason, 1994) and SOLVEQ (Reed and Spycher, 1989). These programs also produce the equilibrium constant, the reaction quotient and saturation index of a given reaction at any given temperature. On the basis of this, a method has been presented by Reed and Spycher (1984), namely the log(Q/K) diagram, showing the state of saturation of many minerals with respect to a given solution composition as a function of temperature. The convergence of log(Q/K) curves for the minerals to zero at some temperature establishes the basis for determining a mineral assemblage and temperature of equilibration of natural geothermal waters, fluid

inclusions, hot spring waters, etc. from the analysis of water alone. The effects of boiling, dilution, temperature variations and lack of equilibrium can be assessed by examining the characteristics of plots. Other effects, such as inaccurate water analyses, and poor thermodynamic data for minerals and aqueous ions and complexes lead to dispersion on such plots and complicated geologic interpretations (Reed and Spycher, 1984).

2.4 Mixing models

The thermal waters ascending from a geothermal reservoir may be cooled by mixing with cold, shallow waters, which tend to occur where there is a change of rock permeability. It is common that the pressure potential in the upflow zones of many geothermal systems is lower than in the enveloping cold groundwater bodies. When this is the case, cold water tends to enter the geothermal system and mix with the rising hot water. Since cold waters are mostly lower in dissolved solids than geothermal waters, mixing is often referred to as dilution with respect to conservative components. However, mixing can upset chemical equilibria between water and rock minerals, thus causing a tendency for the water to change composition after mixing with respect to reactive chemical components, which may yield misleading results of geothermometers (Arnórsson, 2000).

At present, there are a few mixing models of geothermal and cold water applied to estimate subsurface temperatures in geothermal systems, which refer to mixing of two components of quite different compositions in such a way that the concentrations of reactive components do not change much after mixing has occurred. Sometimes, mixing at deep levels in geothermal reservoirs is likely to be completely masked for reactive constituents through re-equilibration of these constituents subsequent to mixing, in which case application of geothermometers is appropriate to estimating subsurface temperature rather than the mixing models.

It is necessary to establish that the sampled and analysed waters are truly mixed before applying mixing models to estimate reservoir temperatures. Recognition of mixed water on the basis of chemical composition of a single sample is generally not convincing, so the mixing process has to be identified and quantified by consideration of samples from many springs or wells and surface waters. Linear relationships between the concentrations of conservative components, such as between Cl and B or Cl and δD, are generally considered to constitute the best evidence for mixing. Sometimes the near linear relations between Cl and $\delta^{18}O$ or chloride and silica have been observed for variably mixed waters in some geothermal fields. Such relationships imply that $\delta^{18}O$ and silica behave as conservative components after mixing (Arnórsson, 2000).

Another method of showing mixing for a larger number of constituents is by using a Schoeller diagram (Truesdell et al., 1987). This diagram compares the log concentrations of fluid constituents from a number of analyses, with constituents of each analysis connected with a line. The effect of mixing with dilute water is to move the line representing an analysis vertically without changing its shape. Slopes of lines between constituents represent concentration ratios. So when many analyses are represented, the pattern of mixing will remain clear. Normally, the thermal waters have higher concentrations of Li, Na, K, F, Cl, SO_4 and B; the cold waters have higher Mg and Ca but have almost the same HCO_3 as the thermal waters. The thermal waters are particularly low in Mg and Ca, which can show the mixing of cold water. This diagram is much more effective than a table in showing this mixing, and serves as an introduction to the water chemistry of the area. When there is an independent indication of mixing, the mixing model can be applied to allow estimation of the hot water component in the reservoir. There are essentially three kinds of mixing models: 1) The chloride-enthalpy mixing model; 2) The silica-enthalpy warm spring mixing model; 3) The silica-carbonate mixing model (Arnórsson, 2000).

2.5 Monitoring of reservoir response to production

Generally, there is a decline in fluid pressure in the reservoir during the production from wells in a geothermal field when withdrawal of the fluid exceeds the natural throughflow rate or natural discharge rate, the extent of which depends on the rock permeability and the rates of fluid extraction and recharge. The pressure drawdown mainly causes wells to become unproductive because of the lack of recharge of thermal water or increase of recharge of cold water into the reservoir (Arnórsson, 2000).

Therefore, it is necessary to monitor chemical and isotopic data on the reservoir because they can provide useful information on the response of the reservoir to the production load as regards recharge. Such data have also proved valuable to map cold water recharge into single liquid water reservoirs and provide information on the quality of the fluid for the use in question, including any changes in scaling and corrosion tendencies (Arnórsson, 2000).

The conservative components, such as chloride, deuterium, B and $\delta^{18}O$ etc., are particularly useful in mapping recharge into exploited geothermal reservoirs, because most of them trace recharge into geothermal reservoirs. However, the relative components will react between themselves and/or with minerals in the rock towards equilibrium as the recharging water gains heat. Since the principal variable for monitoring studies is time, it is convenient to present chemical data from discharged fluids as plots against time where time is on the x-axis and the respective chemical component concentration or ratio on the y-axis. Both primary data and derived data can be plotted to show the possible trend of change of the reservoir (Arnórsson, 2000).

3. INTERPRETATION OF THERMAL FLUIDS FROM STRANDIR AREA, NW-ICELAND

3.1 Background

The NW-peninsula of Iceland, Vestfirdir (Westfjords), is far from the active volcanic belts. This area consists primarily of tholeiitic basalts of Miocene age, 15-10 Ma, and the general structural grain, as represented by dikes and faults, is NE-SW (Moorbath et al., 1968; McDougall et al., 1984). The research area is in the younger part of the Miocene series. On this peninsula, there are many thermal springs ranging in temperature from near boiling to just above ambient. The distribution of low-temperature activity in Iceland can, to a large extent, be correlated with the major active tectonic features of the country. This is the case for northern, western and southern Iceland, but is less clear in Vestfirdir as geological data are too limited to verify such a correlation. In this section, a few samples from the thermal springs and boreholes in the Strandir area, the eastern part of Vestfirdir are collected, and interpreted using the geochemical methods described above in order to evaluate characteristics of the geothermal fluids in this area.

3.2 Sampling and analysis

In this study, a total of 10 samples from the representative hot springs and geothermal boreholes were selected. The hot springs are located in Goddalur (Samples 7 and 8), Asparvík (Samples 2 and 3), Gvendarlaug (Sample 1), Ásmundarnes (Sample 4) and Bakki (Sample 9). The geothermal boreholes include KL-4 (Sample 5) and DN-7 (Sample 6). Sample 10 is from a groundwater borehole in Drangsnes. The collected sample locations are shown in Figure 1.

The samples were mostly collected in the 1970's except Sample 10, which was collected in 1997, and they were all analysed in the chemical laboratory of Orkustofnun, Iceland. The results of these sample analyses are listed in Table 2.

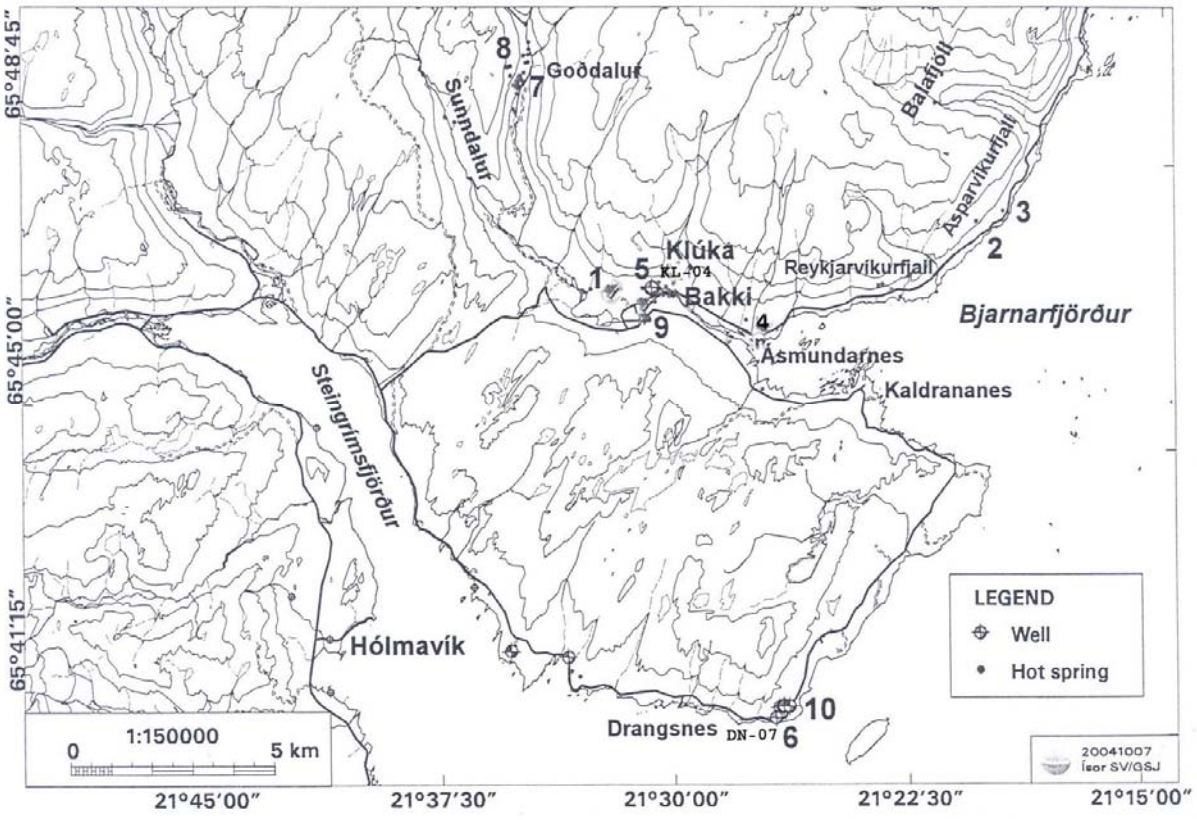

FIGURE 1: The location of sampling points in the Strandir area

TABLE 2: The chemical analyses of samples from NW-Iceland (in ppm)

Sample no.	Type	Location	Number	Temp. (ºC)	pH	Na	K	Mg	Ca	Cl	SO_4	CO_2	SiO_2	F	TDS
1	Spring	Gvendarlaug	19793062	40	9.91	26.9	0.25	0.01	2.49	15.6	6.5	17.3	33.1	0.11	162
2	Spring	Sveinanes	19760269	19	10	22.8	0.08	0.02	3.1	15.3	7.3	10.4	15.9	0.065	92
3	Spring	Asparvík	19780065	11	9	16.3	0.162	0.49	3.3	13.1	4.3	10.8	17.5	0.05	60.8
4	Spring	Ásmundarnes	19760274	31.8	10.07	25.1	0.16	0.01	2.24	16.6	6.4	13	27	0.063	106
5	Well	KL-04	19760275	-	10.22	31.5	0.23	0.02	2.14	16.9	7.6	10.6	42.6	0.098	132
6	Well	DN-7	97-0481	58.4	9.42	131	1.82	0.008	19.1	183.5	41.9	8.72	83	0.32	507
7	Spring	Goddalur	19770204	54.8	10.16	38.2	0.33	0.01	1.7	17.8	7.92	13.4	55	0.21	138
8	Spring	Goddalur	19760277	58.2	10.21	36.7	0.39	0	1.8	18	7.1	13.3	57	0.16	163
9	Spring	Bakki	19760273	29.8	10.17	34.5	0.17	0.02	1.71	18.5	8.2	13.7	38	0.13	134
10	Cold water	Drangsnes	97-0482	6.9	7.71	21.1	0.52	2.76	14.9	33.5	6.46	39.8	14.8	0.11	126

The maximum measured temperature is 58.4ºC and the minimum is only 11ºC; pH values and TDS are mostly above 10 and below 170 ppm, respectively, except Sample 6. The lower TDS and higher pH is attributed to the high reactivity of basaltic minerals as well as the generally limited supply of CO_2 from the organic sources to surface water (Arnórsson, 1995). However, the relative higher TDS of Sample 6 is reflected in higher concentrations of Cl, SO_4, Na, K, probably resulting from the origin of deep source or the mixing of seawater (Arnórsson, 1995). Sample 10 represents the ground water, characteristic by low pH value, high Mg, Ca and CO_2 etc.

3.3 Classifications of samples

Firstly, the samples should be classified before they are further studied by other geochemical methods. Here, all the samples are plotted in the Chebotarev diagram shown in Figure 2. Most of the samples are located in the upper left area of the diagram and belong to chloride-bicarbonate waters, showing a

thermal water source with relatively high content of NaCl, or sea water source sometimes. It is noteworthy that Sample 6 is far from the others, falling in the range of chloride waters, indicating a different source. Sample 10 is in the area of alkali bicarbonate, indicating high content of groundwater. The Cl-SO_4-CO_3 ternary diagram shows similar results (Figure 3). Sample 6 is close to the Cl corner, and Sample 10 is located in the area of peripheral waters. Other samples are plotted in the area between peripheral waters and mature waters, indicating that most of these samples are probably a mixture of thermal water and groundwater.

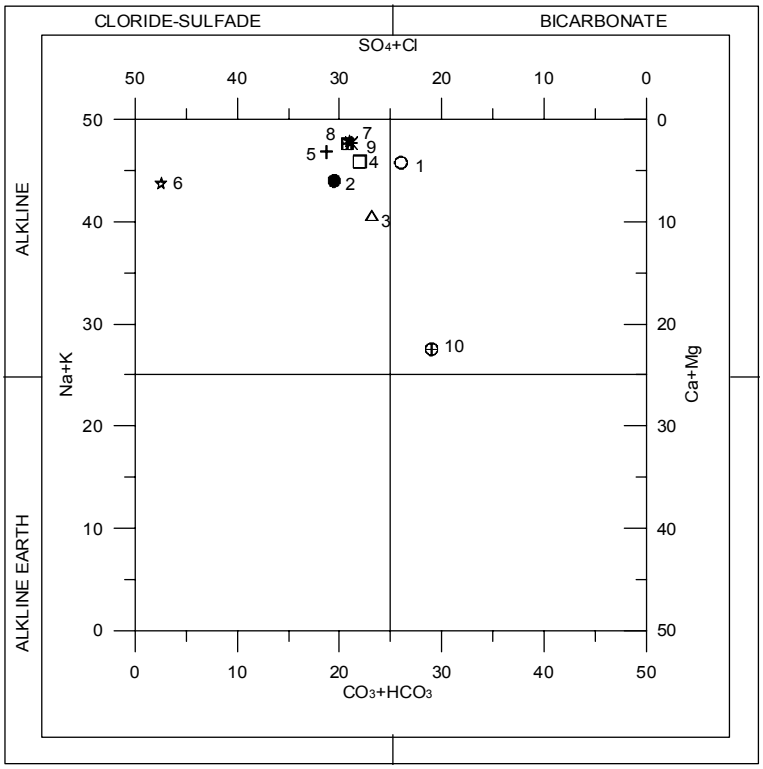

FIGURE 2: Chebotarev diagram showing the classification of samples from the Strandir area

3.4 Geothermometry

Subsurface temperatures are predicted by the calculations of various geothermometers and are listed in Table 3.

Chalcedony temperatures vary in the range of 22-100°C, close to the measured temperatures, regarded as the better indication of subsurface temperatures (Arnórsson, 1995). The temperatures from those involving Ca are too high, probably because of the effect of CO_2. The Na-K geo-thermometers show different temperatures by the use of equations in Table 1, of which the temperatures from Fournier (1983), 35-92°C, are a little higher than chalcedony temperatures, probably indicating information on a deeper source.

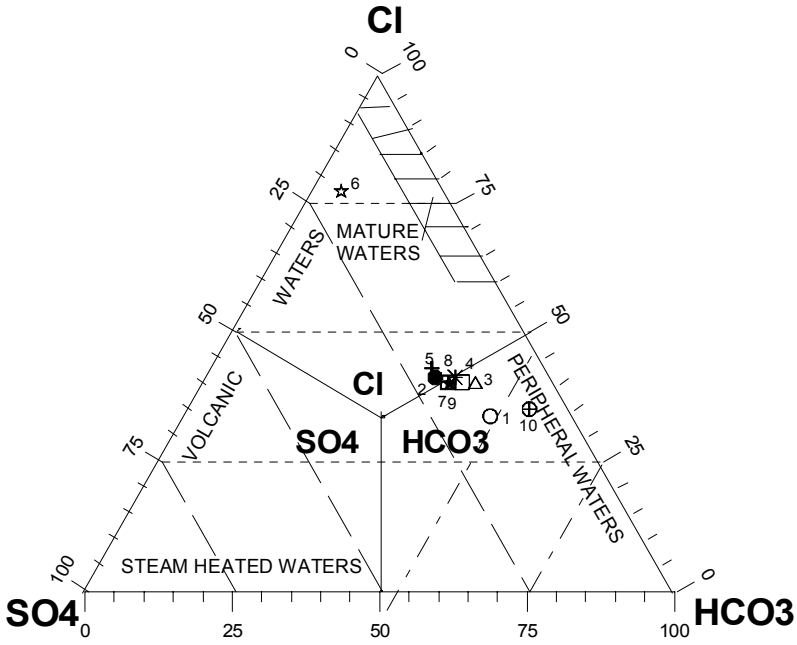

FIGURE 3: Cl-SO_4-HCO_3 ternary diagram showing the classification of samples from the Strandir area

The thermal samples are plotted in a Na-K-Mg triangular diagram to show that most of the samples are close to fully equilibrated except Point 8, and the subsurface temperatures are all below 100°C except Sample 6, which reaches 100-120° (Figure 4). Besides, most of the data are close to the corner of Mg, probably resulting from the mixing of groundwater.

TABLE 3: The geothermometer temperatures in NW-Iceland (ºC)

Sample no.	Type	Temp. (°C)	T1	T2	T3	T4	T5	T6	T7	T8	T9	T10
1	Spring	40.0	83.5	52.4	23.2	35.3	73.1	94.4	252.0	-50.1	320.2	140.9
2	Spring	19.0	55.0	22.7	-14.7	-2.5	35.9	57.4	169.8	31.2	284.2	97.7
3	Spring	11.0	58.5	26.2	26.2	38.3	76.0	97.3	200.3	116.8	242.4	119.9
4	Spring	31.8	75.1	43.5	7.3	19.5	57.7	79.1	224.5	-30.7	317.9	126.3
5	Well	-	94.5	64.0	12.8	25.0	63.1	84.5	257.2	-31.4	354.6	140.6
6	Well	58.4	127.0	99.3	42.2	54.2	91.2	112.2	351.9	219.1	410.9	181.9
7	Spring	54.8	106.3	76.7	19.9	32.1	70.0	91.3	303.8	95.9	406.7	159.8
8	Spring	58.2	108.0	78.6	29.3	41.4	78.9	100.1	314.2	-	394.4	165.7
9	Spring	29.8	89.4	58.7	-2.6	9.5	47.9	69.4	248.2	50.9	388.0	133.4

Note: T1-T10 refer to Table 1.

3.5 Log(*Q/K*) diagram

According to the chemical components measured in the laboratory, the properties of aqueous solutions in deep reservoirs are calculated by WATCH (Arnórsson et al., 1983; Bjarnason, 1994) and the log(*Q/K*) vs. temperature diagrams are plotted in Figure 5. Considering the compositions of basalts and commonly observed secondary minerals, 5 types of minerals are selected to show their equilibrium with the solutions, anhydrite, calcite, chalcedony, albite-low and microcline, but due to the lack of aluminium data, most diagrams only display the former 3 non-aluminous minerals except Samples 1 and 6. The details are described below:

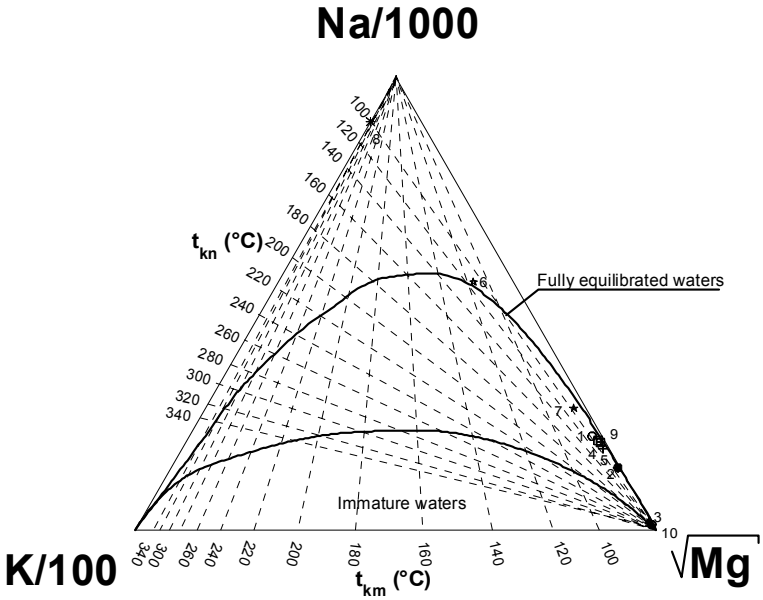

FIGURE 4: Na-K-Mg ternary diagram of samples from the Strandir area

As Sample 1 illustrates, the curves of minerals do not cluster at one temperature. Chalcedony, albite-low and calcite, intersect the log(*Q/K*) = 0 axis at 42°C, which is close to the measured temperature; microcline attained equilibrium at 55°C or so, and anhydrite is undersaturated in the range of reference temperatures. All these minerals appear to have a downward shift, and compared with the geothermemoter temperatures of chalcedony and Na-K, 52.4 and 73.1°C respectively, these equilibrium temperatures are a little lower, which are probably the effect of dilution of ground water (Reed and Spycher, 1984).

Sample 6 displays similar mineral equilibrium curves as Sample 1. Most of the minerals show an equilibrium temperature between 70 and 90°C, still lower than the geothermometer temperature of chalcedony and Na-K, 99.3°C and 91.2°C, respectively, but higher than the measured temperature of 58.4°C. In addition, the curves still seem to shift downwards, and most minerals are supersaturated at the measured temperature, probably attributable to the mixing of sea water.

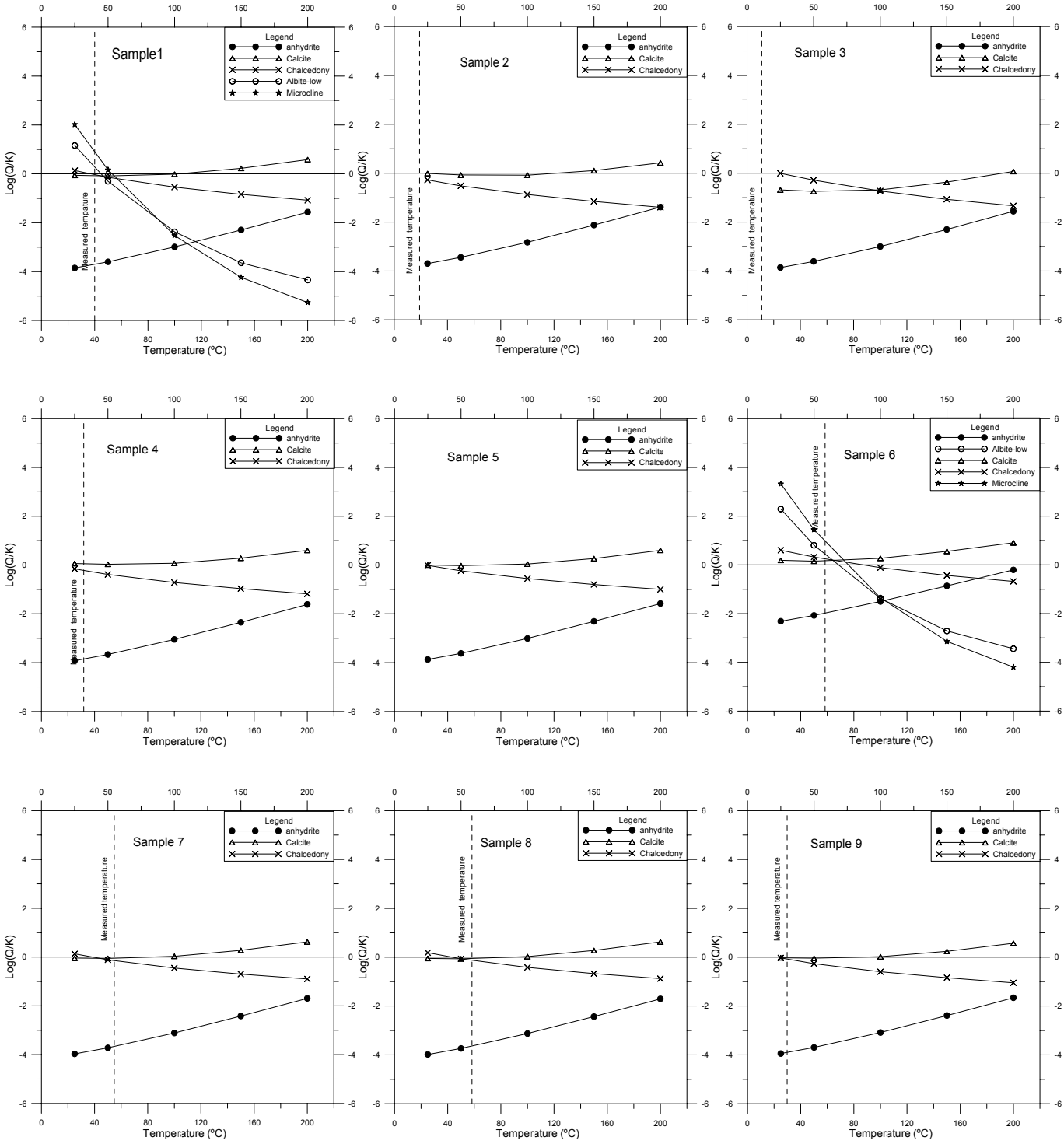

FIGURE 5: Saturation states of selected minerals with respect to samples from the Strandir area

The other samples, short of low-albite and microcline curves, only supply simple information. Samples 2 and 3 have lower measured temperatures and all mineral curves have large shifts downwards, indicating significant dilution of ground water. Samples 4, 5, 7, 8 and 9 also have traces of dilution, but to a lesser extent.

3.6 Mixing model

The main components of the samples are plotted in a Schoeller diagram (Figure 6). Most components of the thermal samples have trends that approach groundwater, like K, Mg, Ca, SiO_2 and F, indicating the mixing of groundwater. Here, the concentration of Cl in groundwater is higher than for most thermal samples, probably because the groundwater has been mixed by seawater. In addition, attention should be paid to Samples 6 and 3. The components in Sample 6 are farthest from groundwater, and those in Sample 3, like Mg and SO_4, are close to it, implying that these samples represent the minimum and maximum mixing with groundwater, respectively.

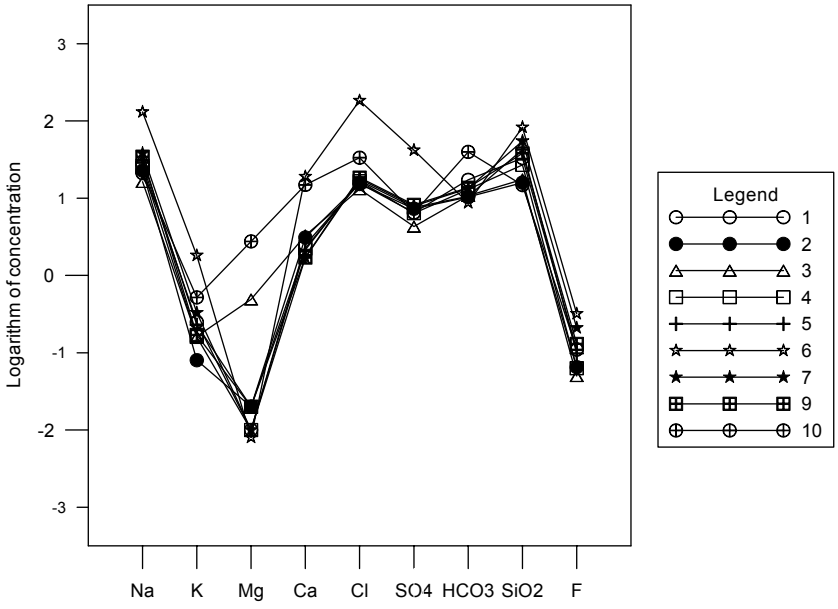

FIGURE 6: Schoeller diagram showing a few components of samples from the Strandir area

Since all the samples appear to be mixed with cold water, the mixing model can be used here to predict the subsurface temperatures in reservoirs. In this case, we use the silica-enthalpy warm spring mixing model.

When applying mixing models, several simplifying assumptions are made. The mass and heat are assumed to be conservative both during and after mixing so that chemical reactions occurring after mixing are considered insignificant and do not modify the water composition. The data points representing the thermal springs and cold water are plotted in the silica-enthalpy diagram (Figure 7). Through the data points, three lines can be drawn. The upper line is connecting Sample 10 (cold water) and Samples 7 and 8 (Goddalur), and extrapolated until it intersects the chalcedony solubility curve, resulting in the predicted temperature of 106ºC; the medium one, through Samples 1 (Gvendarlaug), 4 (Ásmundarnes) and 10 (cold water), produces the subsurface temperatures of 62ºC; the low one, from Sample 10 to Sample 3 (Asparvík), corresponds to 24ºC. The results are mostly in agreement with the geothermometer temperatures of chalcedony except Samples 7 and 8, confirming that most fluids in this area are mixed by groundwater.

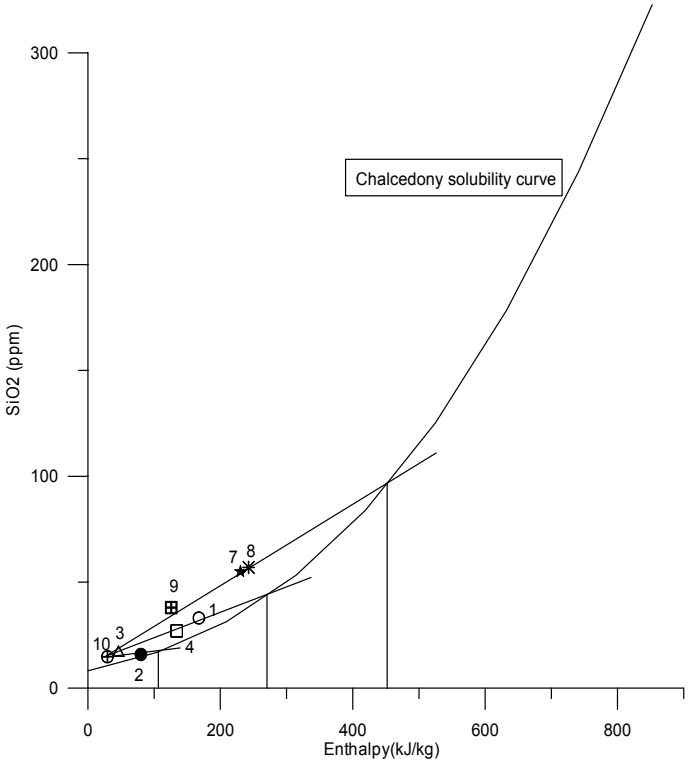

FIGURE 7: SiO_2-enthalpy mixing models for samples from the Strandir area

3.7 Summary

Samples from hot springs and boreholes located in the Strandir area, NW-Iceland, mostly belong to chlorite-bicarbonate waters except one from the Drangsnes field (Sample 6), which belongs to chlorite waters and close to mature waters, probably mixed by seawater. The subsurface temperatures in this area are 22-100°C, according to the chalcedony and Na-K geothermometers (Fournier, 1977; 1983). Most of these fluids are probably diluted by groundwater, and the Asparvík field (Sample 3) showed the maximum extent. The equilibria between minerals and fluids are mostly not attained.

4. APPLICATION OF GEOCHEMICAL METHODS IN THE LIANGXIANG FIELD

4.1 Location and terrain

The Liangxiang field is located in the Fangshan district, Beijing, about 20 km southwest from the urban centre and 15 km northeast of the series of mountains (Figure 8). The altitude of the area decreases from northwest to southeast, with an average elevation of 50 m above sea water (Xiang et al., 2000).

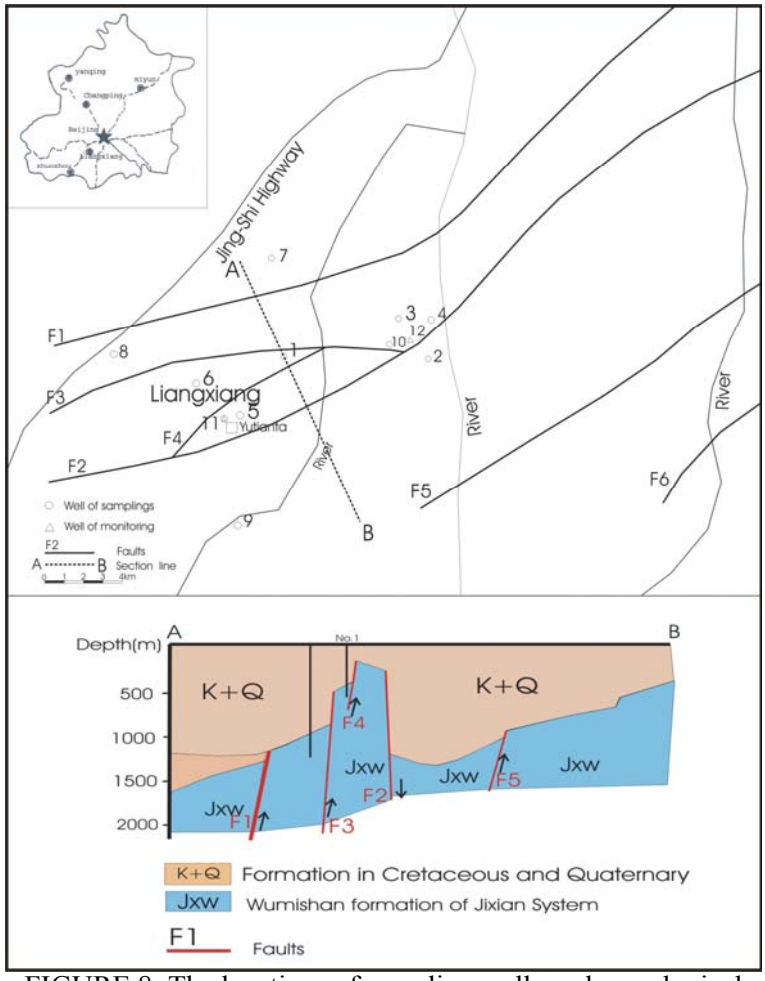

FIGURE 8: The locations of sampling wells and a geological cross-section in the Liangxiang geothermal field

4.2 Geothermal geology

As far as the regional geological setting are concerned, Liangxiang geothermal field is situated in the southwest area of the Beijing Graben, which extends in a SW-NE direction, bordered by Huangzhuang - Gaoliying fracture and Nanyuan-Tongxian fracture. The basement of the graben, the main geothermal reservoir, is siliceous dolomite of the Jixian System (Middle Proterozoic group), which is buried at the maximum depth of about 4000 m along the axis of the graben. The Liangxiang area, located in an uplift zone of the structure, has a clear local geological setting. According to the data from drilling logs, there is only one reservoir exploited, namely the Wumishan formation (Jx.w) of the Jixian System, which is distributed in the whole field and consists of siliceous dolomite rock deposited about 1.2-1.4 billion years ago, with a thickness of more than 2000 m. So far, no drillings have penetrated below this formation. Above the reservoir, there are mainly strata formed successively in the Cretaceous, Tertiary and Quaternary periods, regarded as caprocks. The Cretaceous formation (K) is composed of conglomerate with dominant grains of base igneous rock and sandstone, which covers most of the area with a thickness up to 1300 m. The Tertiary formation (E-N) is a fragment of sandstone and igneous rock and it was found to be only 200 m thick in the well in the east of the field. The surface layer is loose clay and sand of

Quaternary (Q) age, with thickness of less than 100 m in the field (Xiang et al., 2000). The relationships of these strata are displayed in the cross-sectional map in Figure 8.

The geothermal field is dominated by 5 faults striking in a SW-NE direction, which control the thickness of the formations. The two largest faults, F1 and F2, extend to the geothermal field and are regarded as the boundaries of the uplift zone. F3 and F4 are secondary faults in this uplift zone, which make the strata nearby the Liangxiang Town go further. According to the data from drillings near Yutian Tower, the reservoir, Jxw, is buried at less than 10 m depth under Quaternary clay (Xiang et al., 2000), suggesting the fluid in the reservoir is probably mixed with groundwater.

4.3 Exploration and utilization of the geothermal resource

The geothermal resources have been developed since a spring of 30ºC was found and an observation well was drilled in the yard of the Liangxiang ceramics factory, producing geothermal water of 36ºC in the 1960s. In the past 40 years, geothermal surveys and explorations have been gradually carried out, including geological, geophysical, geochemical and exploration drillings. So far, more than 20 wells have been drilled with a temperature range of 36-60ºC, supplying the basic data of geothermal conditions in this field. The distribution of subsurface temperature is controlled by a few thermal faults and different formation temperature gradients. In this area, the average temperature gradient of the reservoir is 1.5ºC /100 m and that of caprocks is 3.5-4ºC /100 m.

The permeability of the reservoir is strongly affected by the faults. The flowrate from wells near F4, when the drawdown is 1 m, is more than 1000 m^3/d, but only 100 m^3/d near F1 and F2, indicating the best permeability in the area is near secondary faults.

At present, the geothermal water is used for swimming, bathing and fish farming etc. The total production reached 1.162 million m^3 in 2003 (He and Rong, 2004). The assessment of geothermal resources in the Liangxiang geothermal field carried out in 2000 defined the area of resources as 68 km^2 and involves the geology, geophysics, geochemistry and calculation of resources etc. The isotopic studies indicated that the geothermal fluid originates from the southwest area of the mountains and flows from the southwest direction to the Liangxiang field (Xiang et al., 2000). In the discussions below, the methods mentioned above will be used to extract more information on the fluid in the reservoir from available data.

4.4 Interpretations of chemical compositions in the Liangxiang field

4.4.1 Sampling and analysis

In general, sampling of geothermal water is carried out at the end of a pump test after drilling. Eleven samples finished were selected for this study and the locations of the wells are shown in Figure 8. All the samples were analyzed in the Beijing Water Quality Analytical Centre Laboratory with national qualification. The analytical methods and the results of chemical analyses are listed in Tables 4 and 5.

TABLE 4: Chemical analytical techniques used for the thermal fluid

Composition	Method of analysis
Na	Atomic absorption spectrometry
K	Atomic absorption spectrometry
Mg	Atomic absorption spectrometry
Ca	Atomic absorption spectrometry
F	Ion selective electrode
Cl	Ion chromatography
SO_4	Ion chromatography
Al	Atomic absorption spectrometry
Fe	Atomic absorption spectrometry
PH	Ion selective electrode
CO_2	Alkalimetry-titration
H_2S	Titration
^{18}O	Mass spectrometry
D	Mass spectrometry

TABLE 5: Chemical composition (in ppm) of thermal waters from wells in Liangxiang field, Beijing

Sample no.	Temp. (°C)	Date	pH	Na	K	Mg	Ca	Cl	SO_4	HCO_3	Al	SiO_2	B	F	TDS
1	40	1995.1	7.88	67.38	10.71	25.3	64.35	35.64	128.6	274.6	-	-	-	4.7	474
2	55	1995.7	7.51	71.29	11.05	23.91	56.83	33.83	129.8	258.7	-	26.69	0.04	5.2	595
3	44	1997.4	7.53	62.26	9.11	27.72	68.14	41.46	140.0	274.6	-	27.80	0.18	4.5	663
4	53	1996.8	7.78	61.15	10.31	23.72	55.73	28.80	130.1	252.6	-	35.74	0.39	5.1	586
5	38	1996.11	7.26	68.39	8.73	29.66	97.13	69.49	134.2	323.4	0.08	28.21	0.13	3.8	609
6	39	1997.7	8.15	65.31	10.8	25.28	64.13	34.36	137.5	247.7	0.07	28.5	-	5.2	483
7	49	1997.9	7.49	92.67	9.45	22.13	55.71	32.81	150.7	274.6	0.06	32.36	0.1	5.8	524
8	43	2001.8	7.40	72.00	12.00	25.9	64.7	40.90	138.0	282.0	0.09	11	-	4.7	643
9	45	2002.10	8.00	67.20	10.20	23.10	63.10	33.00	121.0	270.0	-	26.85	0.16	4.9	595
10	48.5	2002.10	7.41	61.70	10.20	23.10	59.50	32.70	116.0	264.0	-	26.80	0.17	5.0	574
11	37	1998.10	-	68.51	8.93	28.58	77.15	57.58	145.0	280.7	0.26	30.92	0.19	4.3	541

The samples were collected in 1995-2002 and measured temperatures are confined to 37-55°C. The pH is in the range of 7-8.5 and TDS is 470-650 ppm. Some components were not analyzed in some samples because the values were too small, such as Al and B.

4.4.2 Classification of natural waters

Figure 9 shows that all of the geothermal samples are confined in the areas of alkali bicarbonate and alkali earth bicarbonate, classified as bicarbonate-chloride waters or chloride-bicarbonate waters. Moreover, if these samples are compared carefully, we can find that samples from the wells in the uplift zone have higher content of groundwater than others, especially No. 5 and No. 11 near Yutian Tower. So it is possible that the fluid in the reservoir of this field has been diluted by more groundwater near Yutian Tower.

The samples are also plotted on the Cl-SO_4-HCO_3 triangular diagram showed in Figure 10. All of the samples fall in the area of bicarbonate waters, and almost converge at one point, showing high contents of groundwater.

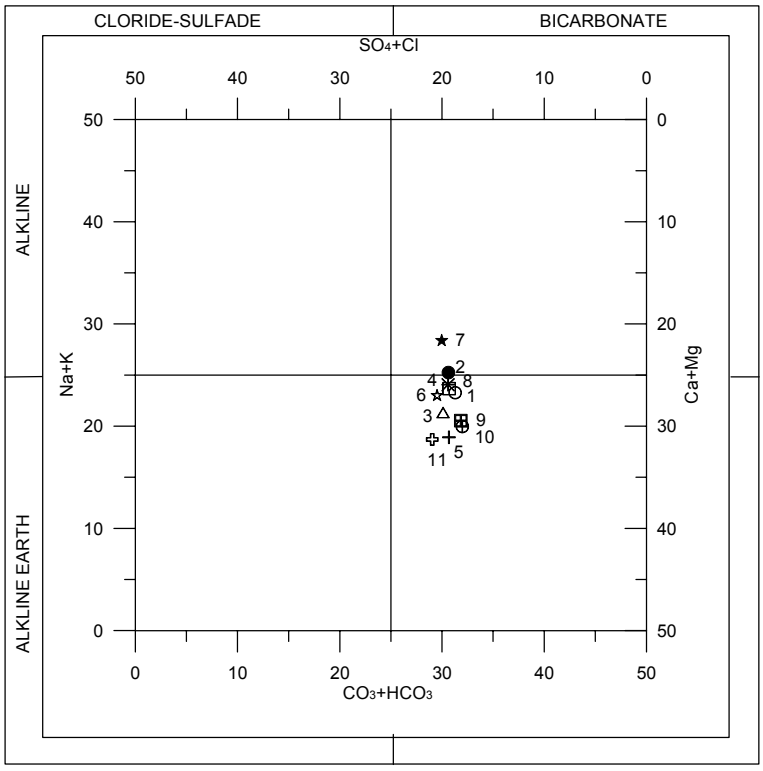

FIGURE 9: Chebotarev diagram showing the classification of samples from the Liangxiang field

4.4.3 Estimation of subsurface temperature

Subsurface temperatures calculated by the various types of geothermometers are listed in Table 6. Geothermometer temperatures formed by quartz and chalcedony vary in the ranges of 74-87°C and 43-56°C, respectively. They seem more suitable than other cation geothermometers, most of which predict too high temperatures, probably because the equilibria have been controlled by clay (Fournier, 1989). Besides, the temperatures calculated by the K-Mg geothermometer are only limited in the 30-40°C range, which is clearly a result of the effect of groundwater.

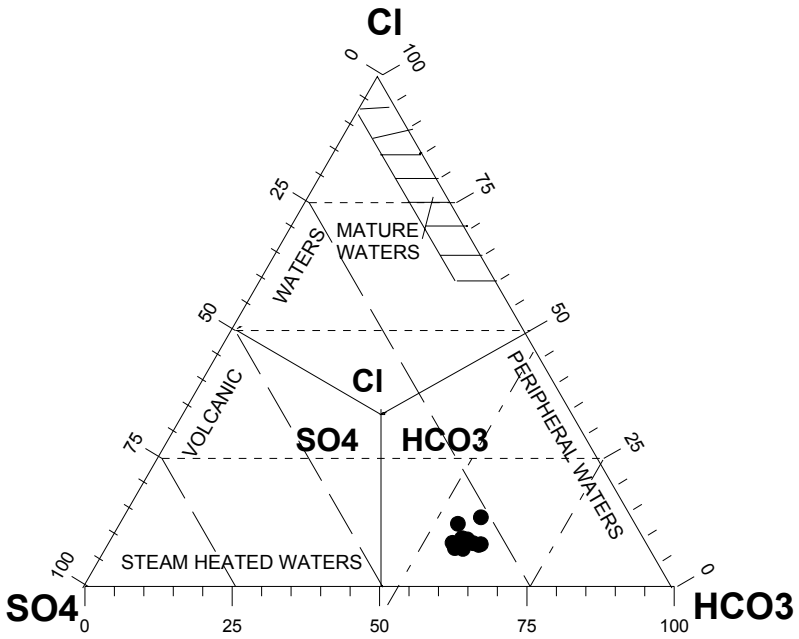

FIGURE 10: Cl-SO_4-HCO_3 ternary diagram showing the classification of samples from the Liangxiang field

TABLE 6: Geothermometer temperatures in Liangxiang field, Beijing (ºC)

Sample no.	Temp. (°C)	pH	T1	T2	T3	T4	T5	T6	T7	T8	T9	T10
1	40	7.88	-	-	243.83	247.57	260.21	272.21	438.8	37.79	235.58	243.51
2	55	7.51	74.65	43.06	240.45	244.41	257.67	269.88	457.11	38.51	248.03	249.18
3	44	7.53	76.29	44.78	232.85	237.33	251.94	264.63	409.87	34.76	224.78	232.32
4	53	7.78	86.78	55.84	251.95	255.12	266.26	277.75	442.31	37.71	233.02	245.55
5	38	7.26	76.89	45.40	215.71	221.29	238.84	252.57	380.70	33.36	216.73	219.99
6	39	8.15	77.30	45.84	249.26	252.61	264.26	275.91	438.92	37.9	232.57	244.12
7	49	7.49	82.54	51.37	189.92	196.99	218.66	233.87	449.36	37.02	279.05	240.34
8	43	7.40	42.37	9.69	250.3	253.6	265.07	276.65	457.01	39.00	242.18	250.27
9	45	8.00	74.89	43.31	237.66	241.82	255.57	267.97	434.03	37.74	236.32	241.19
10	48.5	7.41	74.82	43.23	249.22	252.58	264.23	275.89	435.45	37.74	230.62	242.94
11	37	-	80.66	49.37	218.27	223.68	240.81	245.38	401.26	34.14	228.10	227.65

Note: T1-T10 refer to the Table 1

In addition, the samples are also plotted on the Na-K-Mg diagram in order to classify the samples and estimate the subsurface temperature (Figure 11). But due to the low temperature and the high contents of magnesium, all the samples are assembled at the corner of Mg, which makes it impossible to get any conclusion.

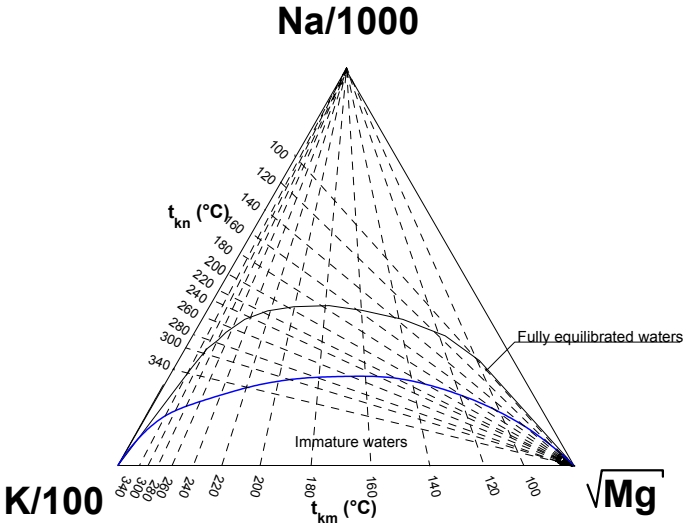

FIGURE 11: Na-K-Mg diagram for samples from the Liangxiang field

4.4.4 Mixing models

Firstly, the extent of mixing with groundwater was evaluated by a Schoeller diagram (Figure 12). The composition of these samples is similar and equal to groundwater with respect to Na, Ca, Cl, and SO_4. F shows the significant difference between geothermal samples

and groundwater, but there is almost no trace of mixing except Sample 5, which shows a trend to be mixed slightly with groundwater.

The contours of concentrations of F and SiO_2 are plotted to illustrate the mixing process and potential area of subsurface temperatures (Figure 13). It is clear that the concentrations of the two components are all higher in the northeastern part as compared to the southwest, implying the good potential of geothermal resources in the northeast of the field. The lower concentrations of F are distributed near sites No. 5 and No. 11, reflecting groundwater flows easily into the reservoir in the uplift zone due to the thinner caprock.

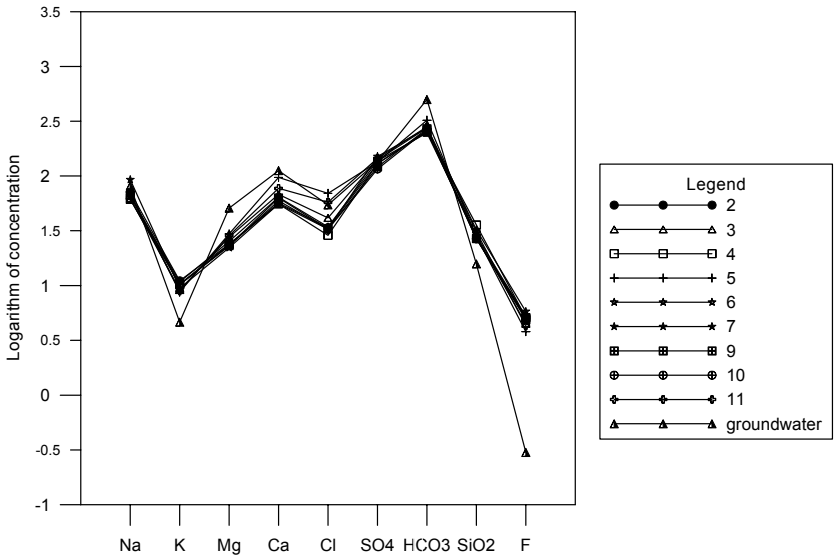

FIGURE 12: Schoeller diagram for samples from the Liangxiang field

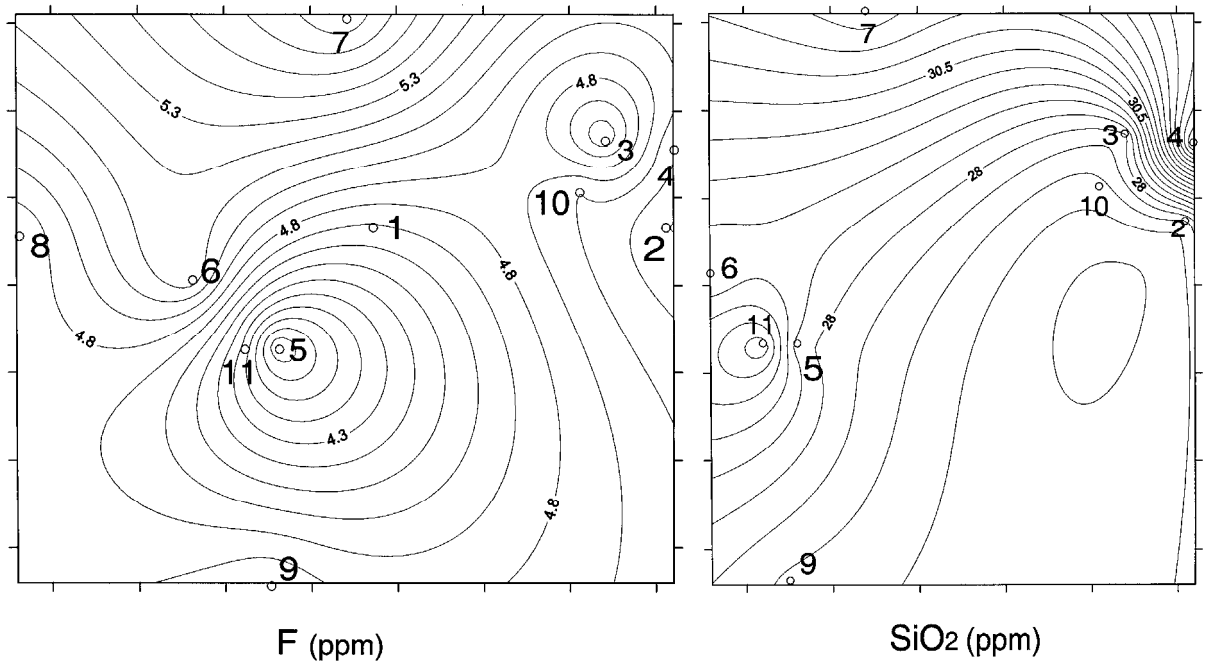

FIGURE 13: Distribution of selected components in the Liangxiang field

4.4.5 Mineral-solution equilibrium

Aqueous species and mineral saturation were calculated by the SOLVEQ program (Reed and Spycher, 1989), but due to the lack of analytical data for some samples, only 7 Log(Q/K) diagrams were generated (Figure 14). Considering that siliceous dolomite is the dominant rock in the reservoir and the lack of valuable Al analyses, 6 types of non-aluminium minerals were selected to show the situation of equilibrium in the system. These are calcite, chalcedony, dolomite, quartz, anhydrite and

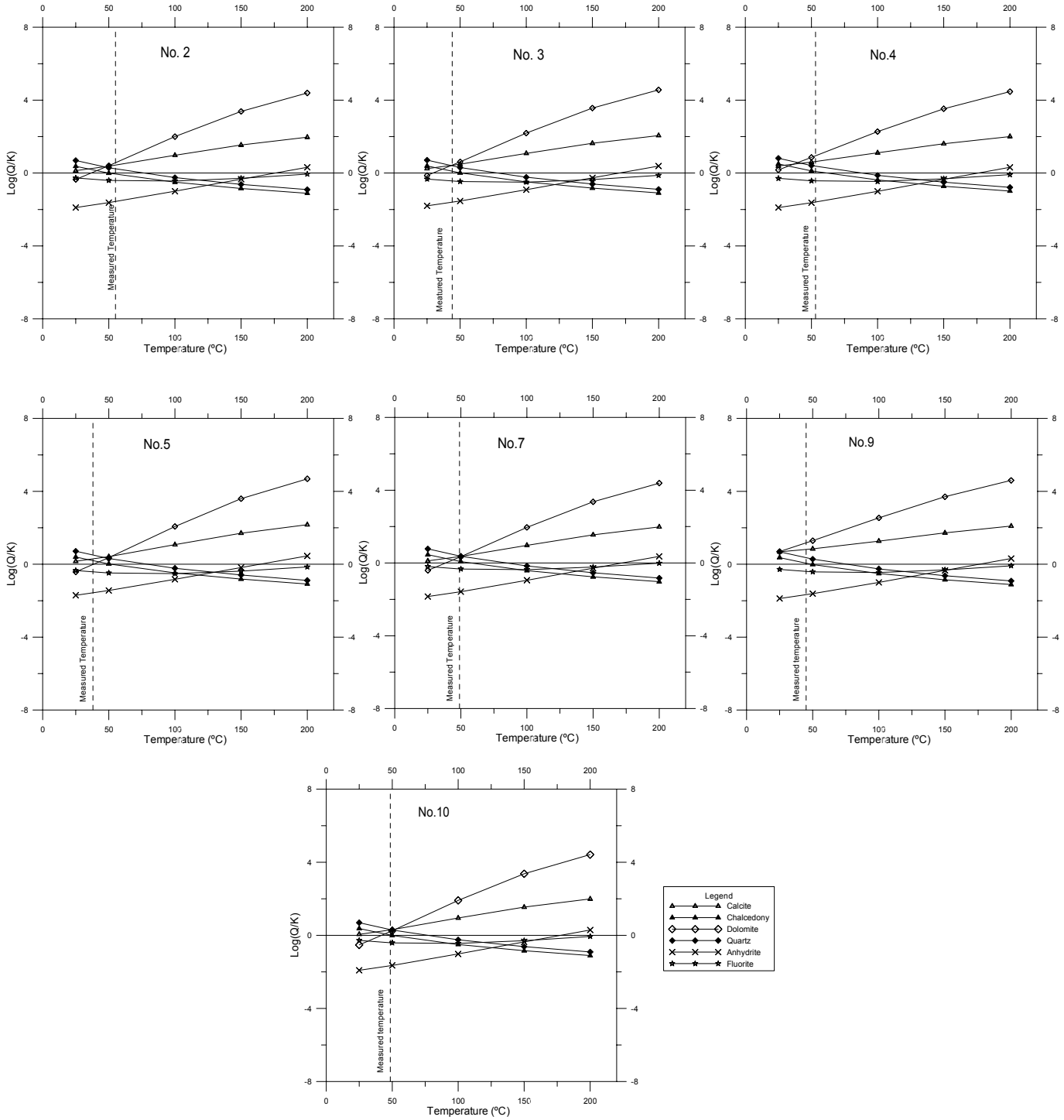

FIGURE 14: Log(Q/K) diagrams for samples from the Liangxiang field

fluorite. These minerals can be divided into two groups. Quartz and chalcedony belong to minerals with prograde solubility which means their solubility increases with increasing temperature. The others have retrograde solubility such as calcite, dolomite, anhydrite and fluorite. The log(Q/K) diagrams have similar patterns. Chalcedony is nearly in equilibrium at the measured temperature, but calcite, dolomite and quartz are always a little supersaturated, and anhydrite and fluorite are under-saturated. The observed supersaturation of calcite at measured temperatures may be attributed to CO_2 loss during sampling and analysis. Much of the 'apparently lost' CO_2 can numerically be added back until the water is saturated with calcite at the measured temperature (He and Reed, 1997). Figure 15 shows the curves of minerals after CO_2 has been added to Sample 2. The calcite and chalcedony

converge at the measured temperature, and dolomite, fluorite and anhydrite are still a little undersaturated, indicating the equilibria between minerals and fluid are not fully attained. On the other hand, the good agreement between measured temperatures and temperatures predicted by the chalcedony geothermometer indicates that chalcedony is controlling the concentration of dissolved silica in the reservoir fluids.

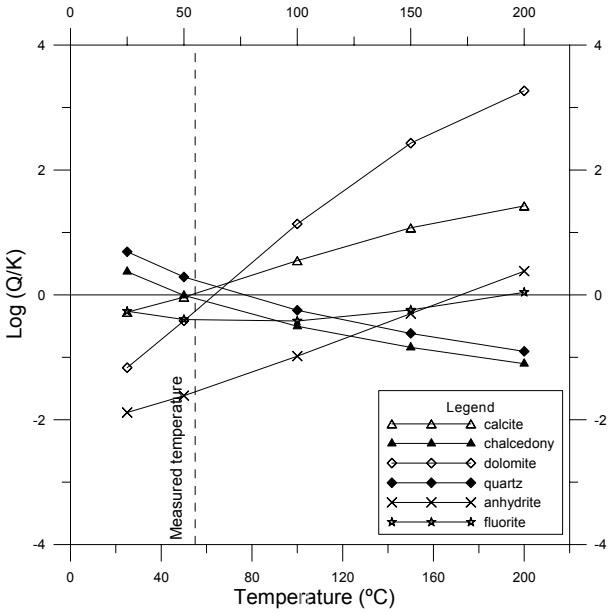

FIGURE 15: Saturation states of some minerals for sample 2 (after adding back CO_2) from the Liangxiang field

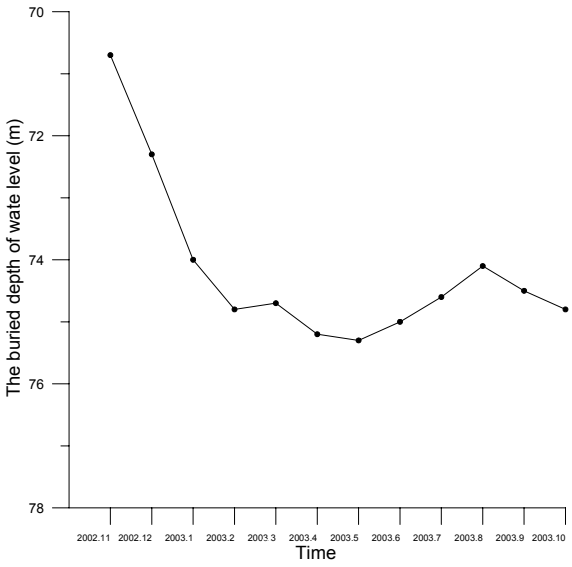

FIGURE 16: The variation of water level in well 13 during 2002.11 - 2003.10, Liangxiang field

4.4.6 Monitoring of the chemical characteristics in the reservoir

In this field, there are only two wells used to monitor the variations in the reservoir. Well 12 is located in the east of the field (Figure 8), near wells 3, 4 and 10, and mainly are used for monitoring of the water level since 1999. Well 11, near Yutian Tower (Figure 8), was drilled in the 1960s and has the shallowest depth of less than 300 m. In order to investigate the reservoir, the monitoring of chemical composition has been carried out in well 11 since the early 1970s, but unfortunately, this was discontinued during the 1980s and in 1993-1997. Figure 16 and Table 7 show the data of water level monitoring, 2002-2003, and chemical compositions, 1990-2003, respectively (He and Rong, 2004).

TABLE 7: Chemical composition of samples (in ppm) from well 11 in the Liangxiang field in 1990-2003

Date	K	Na	Ca	Mg	HCO_3	SO_4	Cl	F	HBO_2	SiO_2	Fe	Al	H_2S
90 11.14	11.30	68.30	74.07	26.88	280.69	134.30	54.40	4.53	0.76	27.00	-	0.0123	0.060
91 03.15	11.10	69.30	71.68	26.36	280.69	134.50	51.60	4.50	2.00	28.00	0.008	0.0015	-
91 11.08	9.77	62.10	74.25	26.62	274.58	136.40	47.10	4.60	0.88	30.00	0.044	0.3590	-
92 03.23	9.52	62.70	70.22	25.92	280.68	133.70	43.50	4.70	1.00	28.00	0.180	0.1601	0.040
92 11.23	9.94	65.00	72.97	26.95	286.78	133.40	46.10	4.70	0.64	30.00	0.236	-	-
98 10.23	8.93	68.51	77.15	28.58	280.70	145.00	57.58	4.30	0.76	30.92	0.016	0.2600	-
99 10.26	9.29	67.57	76.15	27.00	286.80	132.40	43.98	4.50	0.60	28.21	0.200	0.0660	-
00 04.13	10.40	68.60	80.20	28.60	286.00	140.00	59.70	4.10	0.70	28.12	0.184	0.1020	0.1
00 10.31	11.00	71.00	74.50	27.70	305.00	124.00	42.60	4.10	0.46	29.69	0.088	0.1330	0.05
01 10.29	11.00	71.00	74.50	27.70	281.00	139.00	52.50	4.10	0.46	28.54	0.088	0.1330	0.08
02 04.22	9.87	64.60	74.10	26.50	271.00	134.00	50.60	4.40	1.10	29.62	0.056	0.0710	0.05
02 11.06	8.98	64.50	74.90	25.50	275.00	129.00	41.70	4.10	0.68	26.70	0.072	0.0810	0.06
03 03.19	13.30	66.20	75.20	26.10	277.00	128.00	43.90	4.10	0.20	30.61	0.680	0.0320	0.05
03 11.24	10.20	68.80	74.10	26.10	287.00	123.00	47.70	4.40	0.60	30.39	0.044	0.0010	0.05

In Figure 16, it is clear that the water level dropped more than 3 m from November, 2002 to June, 2003 and then rose again from April to August, 2003, which results from the increase of geothermal production in winter. Chemical compositions are regarded as functions of time and the variations of concentrations of Cl, B, HCO_3, Mg, Ca, and geothermometry temperature calculated by chalcedony from 1990 to 2003 are plotted in Figure 17. From these plots, the following changes are seen in the reservoir over time: a) Most components have fluctuated slightly, but the average values have kept

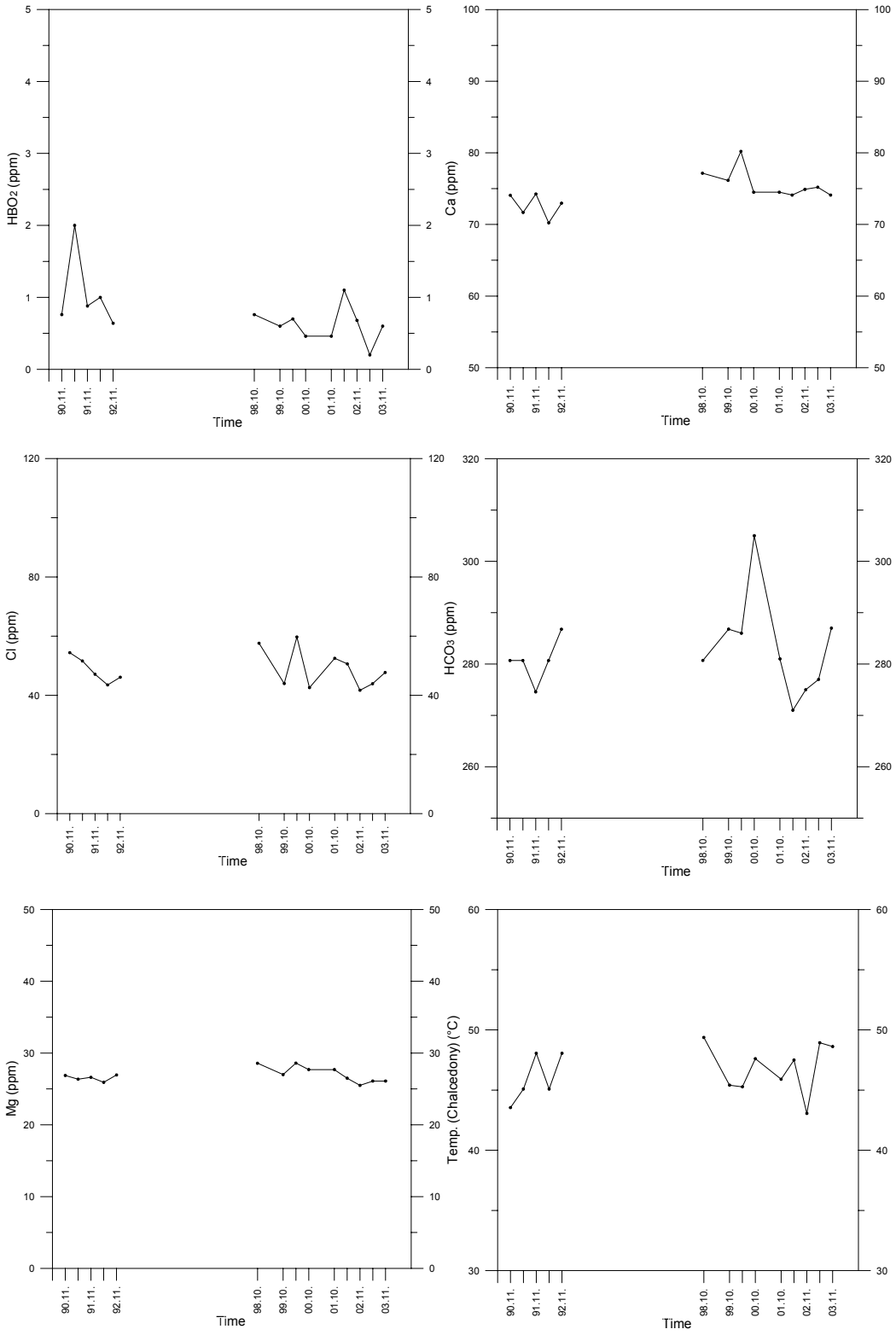

FIGURE 17: The variations of selected components in well 11, Liangxiang field

constant since 1990; b) the geothermometer temperatures of chalcedony vary a little, but there is no indication of a decrease of subsurface temperature during this period. This shows stable recharge of thermal water and, therefore, good potential of geothermal resources in the field.

As is discussed above, since well 11 is located in the groundwater recharge region, the chemical composition of waters from this well responds to the mixing more easily than waters from other wells. So it is important to continue monitoring the well to predict and manage the reservoir in the Liangxiang field in future.

4.4.7 Summary

The Liangxiang field in Beijing is a typical, low-temperature sedimentary geothermal area. The thermal samples are all from wells with temperatures of 35-55°C and their chemical properties are fairly homogenous. The fluid is classified as bicarbonate waters and the subsurface temperature is 43-56°C according to the chalcedony geothermometer. There is no trace of mixing with groundwater in the field except Sample 5, near the area of Yutian Tower. So a simple geochemical model in this field seems to be established: the fluid originates from the meteoric water in the area of the mountains in the southwest; it penetrates to the deep strata and flows to the field; on the way, it gains the heat and reacts with the bedrock; in the field, the deep fluid rises along the fractures, and is mixed slightly with groundwater in the area near Yutian Tower; the equilibria between most of the minerals and fluids are not attained probably because of the rapid recharge of geothermal fluids.

The chemical properties of the fluid in the reservoir have not changed much during exploitation since 1990, but the water level was lowered with the increase of production during these years. So monitoring should be strengthened to control and manage the exploitation of geothermal resources in the Liangxiang field in future.

5. CONCLUSIONS

Some geochemical methods have been applied to the low-temperature areas of Strandir, Iceland and the Liangxiang field, Beijing, China. They mainly concentrate on the classification of waters, the prediction of subsurface temperature, the study of mixing with cold water and evaluation of mineral-solution equilibria.

The samples from hot springs and boreholes located in the Strandir area, NW-Iceland, supply the information on the geothermal fluids below:

- The geothermal fluids in most of the fields belong to chlorite-bicarbonate waters in a Chebotarev diagram and a Cl-SO_4-HCO_3 triangle diagram except Drangsnes field (Sample 6), which belongs to chlorite waters and is close to mature waters, probably mixed by seawater.
- The subsurface temperatures in this area are 22-100°C, according to the chalcedony (Fournier, 1977) and Na-K (Fournier, 1983) geothermometers, which are regarded as reasonable.
- Most of the fluids are probably diluted by groundwater and the equilibria are not attained, showed by the log (Q/K) diagrams.
- Asparvík field (Sample 3) shows the maximum trace of mixing with cold water and DN-7 (Sample 6) minimum in a Schoeller diagram.
- The silica-enthalpy mixing model indicates the following subsurface temperatures: Goddalur field (Samples 7 and 8) is 106ºC, Gvendarlaug (Sample 1) and Ásmundarnes (Sample 4) are 62ºC, and the Asparvík (Sample 3) field is 24ºC.

The study in Liangxiang field, Beijing shows the following fluid characteristics:

- The fluid is classified as bicarbonate-chloride or chloride-bicarbonate waters in a Chebotarev diagram, and bicarbonate waters in a Cl-SO_4-HCO_3 triangular diagram.
- The subsurface temperature is 43-56°C according to the chalcedony geothermometer (Fournier, 1977), which is in agreement with measured temperatures and regarded as the better geothermometer in this field.
- The Na-K-Mg triangular diagram is not suitable in the field because of the higher concentration of Mg in the collected samples.
- In terms of a Schoeller diagram and distributions of some components, the fluid in the reservoir has no trace of mixing with groundwater except Sample 5, near the area of Yutian Tower, where slight mixing occurred. In addition, the good potential areas of geothermal resources are located northeast of the field because of the higher concentrations of F and SiO_2 there.
- The equilibria between minerals and fluid are not attained fully in the log (Q/K) diagrams.
- The chemical properties of the fluid in the reservoir have not changed much during the exploitation since 1990, but the water level was lowered with the increase of production during these years.

ACKNOWLEDGEMENTS

I am very grateful to the administration of the UNU Geothermal Training Programme in Iceland, particularly Dr. Ingvar B. Fridleifsson, for giving me the great opportunity to attend this training; Mr. Lúdvík S. Georgsson, for helping me with all technical support; and Mrs. Gudrún Bjarnadóttir, for her kindness and efficient assistance during this training. I am also thankful to my supervisors, Mrs. Vigdís Hardardóttir and Mr. Magnús Ólafsson for their good guidance and help for my paper. Thanks also to Dr. Halldór Ármannsson and Dr. Thráinn Fridriksson for their advice to my paper. I would also like to express gratitude to the Geothermal engineering department, Beijing for support of the paper. Finally, I convey my good wishes to all of them and the other UNU Fellows during this training programme.

REFERENCES

Arnórsson, S., 1995: Geothermal systems in Iceland: Structure and conceptual models II. Low-temperature areas. *Geothermics, 24*, 603-629.

Arnórsson, S. (ed.), 2000: *Isotopic and chemical techniques in geothermal exploration, development and use. Sampling methods, data handling, interpretation*. International Atomic Energy Agency, Vienna, 351 pp.

Arnórsson, S., Gunnlaugsson, E., and Svavarsson, H., 1983: The chemistry of geothermal waters in Iceland III. Chemical geothermometry in geothermal investigations. *Geochim. Cosmochim. Acta, 47*, 567-577.

Bjarnason, J.Ö., 1994: *The speciation program WATCH, version 2.1.* Orkustofnun, Reykjavík, 7 pp.

Chebotarev, I.I., 1955: Metamorphism of natural waters in the crust of weathering. *Geochim. Cosmochim. Acta, 8,* Part 1: 22-48. Part 2: 137-170. Part 3: 198-212.

Dall´Aglio, M., Martini and M., and Tonani, F., 1972: *Rilevamento geochimico delle emanazioni vulcaniche dei Campi Flegrei* (in Italian). La Ricerca Scientifica, papers CNR. no. 33, 152-181.

Fouillac, C. and Michard, G., 1981: Sodium/lithium ratios in water applied to geothermometery of geothermal reservoirs. *Geothermics, 10,* 55-70.

Fournier, R.O., 1977: Chemical geothermometers and mixing model for geothermal systems. *Geothermics, 5,* 41-50.

Fournier, R.O., 1983: Self-sealing and brecciation resulting from quartz deposition within hydrothermal system (abs.). *Proceedings of the 4th International Symposium on Water-Rock Interaction, Japan*, 137-140.

Fournier, R.O., 1985: The behaviour of silica in hydrothermal solutions. *Rev. Econ. Geol., 2,* 45-61.

Fournier, R.O., 1989: *Lectures on geochemical interpretation of hydrothermal waters*. UNU-GTP, Iceland, report 10, 73 pp.

Fournier, R.O. and Marshall, M.L. 1983: Calculation of amorphous silica solubilities at 25ºC to 300ºC and apparent cation hydration numbers in aqueous salt solutions using the concept of effective density of water. *Geochim. Cosmochim. Acta, 47*, 587-596.

Fournier, R.O., and Potter, R.W. II, 1982a: An equation correlating the solubility of quartz in water from 25ºC to 900ºC at pressures up to 10,000 bars. *Geochim. Cosmochim. Acta, 46,* 1969-1974.

Fournier, R.O., and Potter, R.W. II, 1982b: A revised and expanded silica (quartz) geothermometer. *Geotherm. Resourc. Counc. Bull., 11-10,* 3-12.

Fournier, R.O., and Rowe, J.J., 1977: The solubility of amorphous silica in water at high temperatures and high pressures. *Am. Min., 62,* 1052-1056.

Fournier, R.O., and Truesdell, A.H., 1973: An empirical Na-K-Ca geothermometer for natural waters. *Geochim. Cosmochim. Acta*, *37*, 1255-1275.

Giggenbach, W.F., 1988: Geothermal solute equilibria. Derivation of Na-K-Mg-Ca geoindicators. *Geochim. Cosmochim. Acta, 52*, 2749-2765.

Giggenbach, W.F., Gonfiantini, R., Jangi, B.L., and Truesdell, A.H., 1983: Isotopic and chemical composition of Parbati Valley geothermal discharges, NW-Himalaya, India. *Geothermics, 12*, 199-222.

Hemley, J.J., 1967: Aqueous Na/K ratios in the system K_2O-Na_2O-Al_2O_3-SiO_2-H_2O. *Annual Meeting Geol. Soc. Amer., New Orleans*, 94-95.

He L.Z, and Rong J.L, 2004: *The report of monitoring and research of geothermal in Beijing, 2003.* Beijing Institute of Geological Engineering, China, report, 15 pp.

He P.Z, and Reed, M., 1997: Theoretical chemical thermometry on geothermal waters: problems and methods. *Geochim Cosmochim Acta, 62-6,* 1083-1091.

Kharaka, Y.K., Lico, M.S., and Law, L.M., 1982: Chemical geothermometers applied to formation waters, Gulf of Mexico and California basins (abs.). *Am. Assoc. Petrol. Geol. Bull., 66,* 588.

Kharaka, Y.K., and Mariner, R.H., 1989: Chemical geothermometers and their application to formation waters from sedimentary basins. In: Naesar, N.D. and McCollon, T.H. (editors), *Thermal history of sedimentary basins.* Springer-Verlag, New York, 99-117.

McDougall, I., Kristjánsson, L., and Saemundsson, K., 1984: Magnetostratigraphy and geochronology of northwest Iceland. *J. Geophys. Res., 89(B8),* 7029-7060.

Moorbath, S., Sigurdsson, H., and Goodwin, R., 1968: K-Ar ages of oldest exposed rocks in Iceland: *Earth and Planetary Science Letters, 4*, 197-205.

Orville, P.M., 1963: Alkali ion exchange between vapour and feldspar phases. *Am. J. Sci., 261,* 201-237.

Reed, M.H., and Spycher, N.F., 1984: Calculation of pH and mineral equilibria in hydrothermal water with application to geothermometry and studies of boiling and dilution. *Geochim. Cosmochim. Acta, 48*, 1479-1490.

Reed, M.H., and Spycher, N.F., 1989: *SOLVEQ: A computer program for computing aqueous-mineral-gas equilibria. A manual.* Department of Geological Sciences, University of Oregon, Eugene, Oregon 37 pp.

Rimstidt, J.D., and Barnes, H.L., 1980: The kinetics of silica-water reactions. *Geochim. Cosmochim. Acta, 44*, 1683-1699.

Tonani, F., 1980: Some remarks on the application of geochemical techniques in geothermal exploration. *Proceedings, Adv. Eur. Geoth. Res., 2nd Symposium, Strasbourg*, 428-443.

Truesdell, A.H., 1976: Summary of section III - geochemical techniques in exploration. *Proceedings of the 2nd U.N. Symposium on the Development and Use of Geothermal Resources, San Francisco, 1,* liii-lxxix.

Truesdell, A.H., Janik, C.J., Goff, F.E., Shevenell, L.A., Trujillo, P.E. Jr., Counce, D.A., Kennedy, B.M. and Paredes, J.R. 1987: The origin of thermal waters of Honduras and puzzling variations in spring chemistries. *Proceedings 9th New Zealand Geothermal Workshop, Auckland, NZ*, 79-88.

Xiang R.Z., Guo Z.L., Ying D.W., Ren W., Zhi W. and Ping J.Z, 2000*: The assessment report of geothermal resources in Liangxiang.* Beijing Institute of Geological Engineering, China, report, 82 pp.